

The Islamic University of Gaza  
Deanery of Graduate Studies  
Faculty of Information Technology



# An Improved Multi-Level Edge-Based Stereo Correspondence Technique for Snake Based Object Segmentation

**Presented by**

**Mohammed Walid Amer**

**Supervised by**

**Dr. Ashraf Alattar**

A Thesis Submitted to Faculty of Information Technology in  
Partial Fulfillment of the Requirements for the Degree of  
Master of Science in Information Technology

2013 - 2014

# Acknowledgment

Thanks and praise to Almighty Allah whose wind has always been at my back to help me produce such a humble work.

My thanks also to my advisor Dr. Ashraf Alattar who helped me to produce this work to light.

Special thanks go to the jury members for their valuable suggestion and comments. I also feel indebted to all my teachers in the Islamic university. I thank them all for their valuable efforts.

My sincere thanks also go to my family specially my father and mother, my brothers and sisters, and my wife and children who motivated, supported and encouraged me to complete this study.

A special thanks to all my colleagues in the UNRWA who helped and supported me to complete this study.

Thanks are also extended to all my friends for their good companionship and support.

# Dedication

To the soul of my brother in his eternal existence.

To my beloved parents.

To my kids, my eye on the future.

To the steadfast Palestinian people.

# Abstract

Disparity maps generated by stereo correspondence are very useful for stereo object segmentation because based on disparity background clutter can be effectively removed from the image. This enables conventional methods such as snake-based to efficiently detect the object of interest contour.

In this research I propose two main enhancements on Alattar's method first I increased the number of edge levels, and utilized the color information in the matching process. Besides a few minor modifications, these enhancements achieve a more accurate disparity map which eventually helps achieve higher segmentation accuracy by the snake.

Experiments were performed in various indoor and outdoor image conditions to evaluate the matching performance of the proposed method compared to the previous work.

**Keywords:** Stereo correspondence, disparity, multi-level edge maps, object segmentation, active contour model, snake, object of interest (*OOI*), region of interest (*ROI*).

## ملخص الرسالة

الدراسة السابقة للعتار والتي تهدف إلى تحسين جودة خرائط الإزاحة (disparity maps) للصور الثنائية (stereo images) بهدف تجزئة عناصر مستهدفة من الصورة، اعتمدت على استخدام خرائط حواف متعددة المستويات (multi-level edge maps) بغرض حصر حسابات المقارنة الثنائية (stereo matching) في الحواف التي تتشابه في القوة، وذلك بهدف تخفيض كمية الحوسبة ورفع مستوى جودة خرائط الإزاحة الناتجة، مما له من أثر واضح في تحسين كفاءة التخلص من الشوائب الخلفية عند فرز عناصر الصورة حسب العمق. في المحصلة يترتب على ذلك تسهيل عمل الطرق التقليدية الخاصة بتحديد الإطار الخارجي للعنصر المطلوب تحديده مثل طريقة نموذج الكنتور النشط (Active Contour Model) أو ما يسمى "Snake" (الأفعى).

في هذا البحث يقترح الباحث اثنين من التحسينات الرئيسية على طريقة العطار، أولهما زيادة عدد مستويات الحواف (edge levels) في خرائط الحواف متعددة المستويات، وثاني هذه التحسينات هو الاستفادة من بيانات اللون في عملية المطابقة، إلى جانب بعض التعديلات الطفيفة الأخرى. هذه التحسينات تنتج عنها خريطة إزاحة أكثر دقة مما يساعد في نهاية المطاف في تطبيق طريقة الأفعى على خلفية خالية من الشوائب مما يعطي تحديداً للعنصر بشكل أكثر دقة.

أجريت الاختبارات على الطريقة المحسنة لتقييم أدائها في ظروف اختبار مختلفة حيث تم استخدام صور داخلية وأخرى خارجية ودرجات متفاوتة من المكونات في خلفية الصورة. كما تم تقييم النتائج بالمقارنة مع الأعمال السابقة وتبين تحسين ملحوظ في دقة خرائط الإزاحة وما يترتب عليه من تحسين في الأداء النهائي لعملية تجزئة العناصر المستهدفة.

# Table of Content

Acknowledgment .....	i
Dedication .....	ii
Abstract in English .....	iii
Abstract in Arabic .....	iv
Table of Content .....	v
List of Figures .....	vi
List of Abbreviations .....	ix
<b>1. Introduction and Literature Review .....</b>	<b>1</b>
1.1) Introduction .....	2
1.2) Literature review .....	6
1.2.1) Snake based object segmentation .....	6
1.2.2) Background clutter problem .....	9
1.2.3) Stereo matching .....	10
2.1.3.1) Correlation measures .....	13
2.1.3.2) Edge-base Stereo matching .....	15
<b>2. Related works .....</b>	<b>16</b>
2.1) Previous works in stereo matching and snake segmentation .....	17
2.2) Previous proposed Method by Alattar .....	21
2.2.1) Generating the Multi-level edge maps from the stereo image pair .....	21
2.2.2) Generating the edge disparity map by the Stereo Matching .....	26
2.2.3) Estimation of the object of interest disparity by target localization .....	27
2.2.4) External energy formulation .....	27
<b>3. The Proposed improved Stereo Correspondence Method .....</b>	<b>30</b>
3.1) Modifying the multi-level edge map .....	33
3.2) Combing multi-level edge maps and color factor to generate the disparity map .....	35
3.3) Estimation of the object of interest disparity by target localization .....	39
3.4) Disparity map filtering .....	41
<b>4. Experiment and Results .....</b>	<b>43</b>
<b>5. Conclusion .....</b>	<b>61</b>
<b>6. References .....</b>	<b>63</b>

## List of Figures

Figure (1.1)	Object Segmentation	2
Figure (1.2)	Active Contour Model (snake)	6
Figure (1.3)	The background clutter problem caused by background edges prevents snakes from accurately converging to the object's boundary- (a) without snake, (b) with snake	9
Figure (1.4)	Stereo matching approach	10
Figure (1.5)	preserving object pixels and eliminating background pixels	11
Figure (1.6)	Stereo Matching	12
Figure (2.1)	(a) Source image – Tsukuba, (b) gradient magnitude map, (c) Edge strength map – $ged(x,y)$ , (d) Multi-level edge map	23
Figure (2.2)	Stereo matching search space reduction. (a) The binary edge map case: the left pixel must be matched against all four pixels on the right, (b) The multi-level edge maps case: the left pixel will be matched with only the first pixel on the right	24
Figure (2.3)	(a) 4-level edge map, (b) 8-level edge map (c) 16-level edge map	25
Figure (2.4)	Edge Disparity Map (left), and <i>LEDM</i> (right)	28
Figure (3.1)	Diagram of our Improved Method	32

Figure (3.2)	Stereo matching search space reduction and accuracy. The multi-level edge maps case: the right pixel will be matched with the pixels that are the same or similar on the left not only with the pixel that is the same.	33
Figure (3.3)	8-level edge map for the Tsukuba image: (a): Right image multi-level edge map, (b): left image multi-level edge map	34
Figure (3.4)	Search space reduction and error reduction. The right pixel will be matched with the pixels similar or less or bigger than pixel on the left by one	37
Figure (3.5)	Stereo matching using the edge strength value and the color factor of the of the edge pixel in the right image with the edge pixel in the left that satisfies the condition in the left image.	38
Figure (3.6)	The ROI of the tsukuba image and its multi-level and color factor disparity map	39
Figure (3.7)	the target localization by using the Bounding Box method	40
Figure (3.8)	The multi-level and color factor disparity map and the layer edge disparity map ( <i>LED</i> M) of the Tsukuba ROI.	41
Figure (4.1)	Results for synthesized clear background images	46
Figure (4.2)	Results for real indoor moderately cluttered background images	47
Figure (4.3)	Results for real indoor clear cluttered background images	48



Figure (4.4)	Results for real indoor slightly cluttered background images	<b>49</b>
Figure (4.5)	Results for real indoor \ cluttered background colored images	<b>51</b>
Figure (4.6)	Results for synthesized cluttered background image	<b>52</b>
Figure (4.7)	Results for real outdoor slightly cluttered background images	<b>53</b>
Figure (4.8)	Results for real outdoor moderately cluttered background images	<b>54</b>
Figure (4.9)	Results for real outdoor highly cluttered background images	<b>55</b>
Figure (4.10)	Results for real indoor highly cluttered background images	<b>56</b>
Figure (4.11)	Results for real indoor slightly cluttered background images	<b>58</b>
Figure (4.12)	Results for real indoor cluttered background images – small OOI	<b>59</b>

## List of Abbreviations:

ROI	Region of interest
OOI	Object of interest
$D_{OOI}$	Disparity value for the object of interest
MLEM	Multi-level edge map
LEDM	layer edge disparity map
ACM	Active contour model
GAC	Geometric Active Contour
GVF	Gradient Vector Flow snake

## **Chapter (1):**

# **Introduction and Literature Review**

This chapter is composed of two sections: 1) introduction, and 2) literature review. In the introduction we present an overview of the problem and the proposed approach. In the second section we present a more detailed discussion of the background.

### 1.1: Introduction:

The goal of object segmentation is to accurately represent the boundary of an Object of Interest (OOI) in an image. As shown in figure (1.1) the object of interest is indicated by surrounding it with a Region of Interest (ROI).

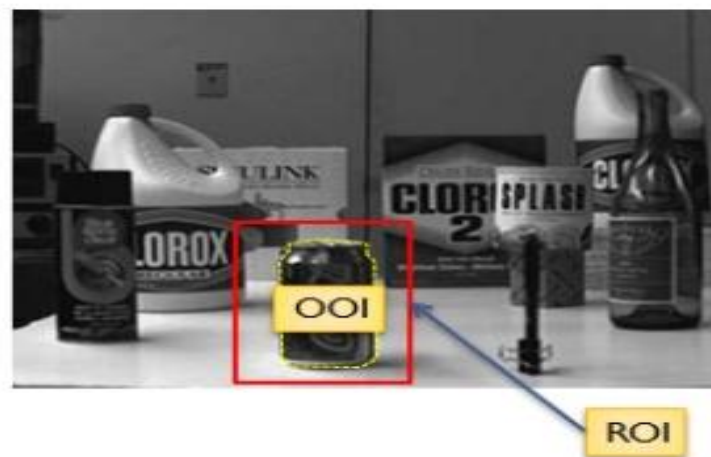


Figure (1.1): Object Segmentation

As will be seen later in the Literature Review section, there are various techniques used for object segmentation in mono images such as the Active Contour Model (ACM or snake) based methods, thresholding [22] and level set technique [21].

Snake-based methods are among the primary methods and are commonly used in applications such as object tracking, shape recognition, segmentation, and edge detection [12]. However, performance of the Snake model degrades significantly when the Snake encounters challenges such as boundary concavities, object occlusion, and background clutter.

The later of these three problems, background clutter, can be largely reduced using the process of stereo correspondence (stereo matching) which can help eliminate non-OOI pixels based on their disparity value. Stereo matching produces a disparity map which gives an estimate the 3D depth of each pixel in the scene. The process involves the pairing of each pixel in the right image with its matching pixel in the left image and registering the difference in location. Based on this disparity map further steps can be taken to filter out the OOI.

Obviously, the accuracy of the segmentation step relies mainly on the quality of the disparity map which relies on the stereo matching technique used. This causal relationship that links object segmentation back to stereo matching is the essential focus of our research.

In the Literature Review section we present the major approaches for stereo matching. One of these approaches is edge-based stereo correspondence which restricts correspondence search to pixels that lie on edges. Many researchers proposed interesting techniques within the edge-based stereo matching approach. Among those, we focus on the work of Alattar reported in [3] which has two important aspects: a) it is tailored for snake-based segmentation, and b) it utilizes the notion of multi-level edge maps. In the literature review we discuss Alattar's work in more details. However, here we only point out that multi-level edge maps are multi-valued (non-binary) edge maps based on the strength of edges. Therefore, a multi-level edge map indicates both edge location and strength. These are two features on which the process of stereo correspondence is based. The advantage of multi-level edge maps over conventional (binary) edge maps is that they allow for reducing correspondence search by enabling the search to be restricted to pixels of similar strength.

My research extends Alattar's work by modifying the number of levels from 4 to 8 levels which leads to higher matching accuracy. Furthermore, I utilize color similarity as a factor in matching estimation. These two modifications increase quality of the disparity map which leads to a more accurate and effective snake-based object segmentation of the *OOI*.

So the main objective of my work is to improve the existing multi-level edge-based stereo matching technique proposed by Alattar and produces a more accurate disparity map leading to more accurate object segmentation by existing snake techniques. This leads me to study and experiment the existing stereo matching method.

To evaluate my work I will evaluate the performance enhancements and drawbacks of the proposed technique under various scenarios and compare with existing techniques.

This thesis is organized as follows. Chapter 1 will give an introduction and a literature review on snake-based object segmentation and edge-based stereo correspondence as well as the Chapters 2 give a related works on the topic and also the previous work by Alattar [3]. Chapter 3 covers the details of our improved object segmentation method. In Chapter 4 the results of applying our method on a set of test images are presented, and the conclusions are given in Chapter 5.

## 1.2: Literature Review:

In this section, we explain the following concepts and the various techniques used for each:

- Snake based object segmentation.
- Background clutter problem.
- Stereo matching.

### 1.2.1) Snake based object segmentation:

Object segmentation is a process performed on an image to extract the exact boundaries of an object of interest (OOI) from the rest of the image. Various applications require object segmentation such as object tracking, shape recognition, segmentation, edge detection, stereo matching. Snakes may be understood as a special case of general technique of matching a deformable model to an image by means of energy minimization [4].

One of the primary techniques for object segmentation is the active contour model (ACM) [4]. An active contour (snake) is an “active” model as it always minimizes its energy functionality and therefore exhibits dynamic behavior. As shown in figure (1.2) the Active Contour Model (snake) is initialized outside the OOI and iteratively converges towards the OOI’s boundary.

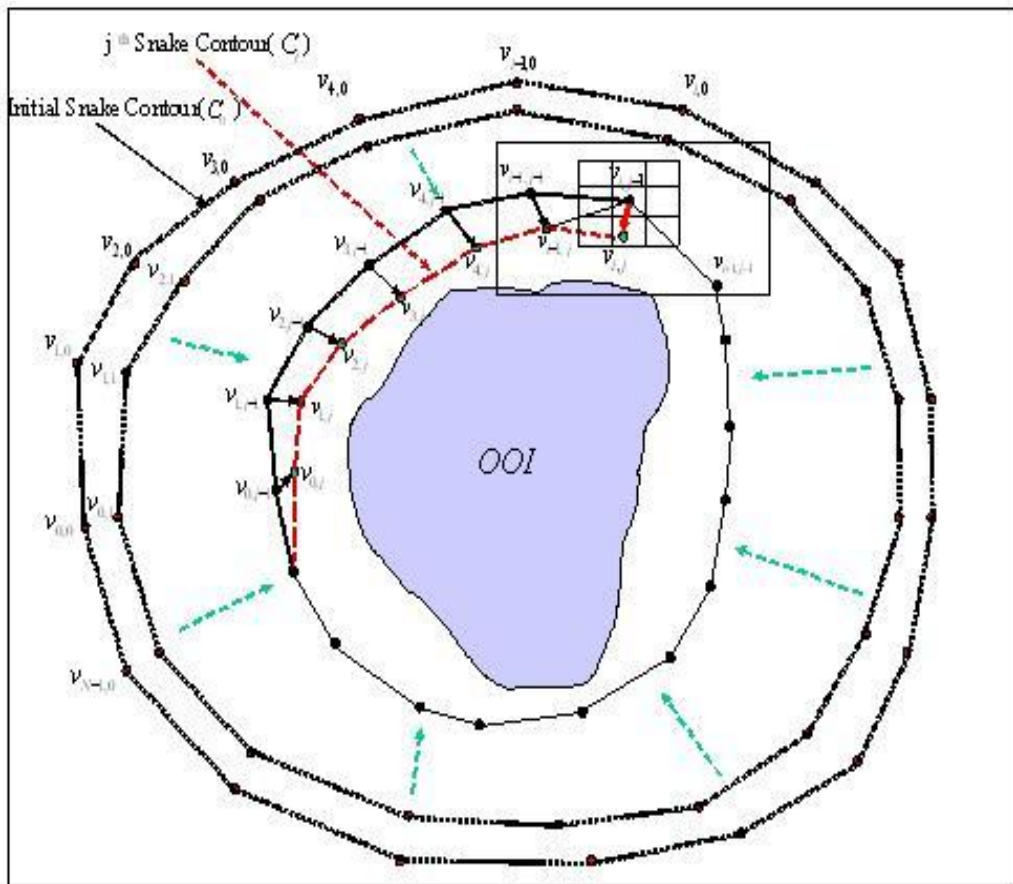


Figure (1.2): Active Contour Model (snake)

One may visualize the snake as a rubber band of arbitrary shape that is deforming with time trying to get as close as possible to the object contour. Snakes do not solve the entire problem of finding contours in images, but rather, they depend on other mechanisms like interaction with a user, interaction with some higher level image understanding process, or information from image data adjacent in time or space. In general, Snake is placed near the object contour. It will dynamically move towards object contour by minimizing its energy iteratively [4].

Object segmentation is accurately representing the boundary of an Object of Interest (OOI) in an image, in order to do so we use the Active contour (Snake) [4] which is an energy minimizing, deformable spline influenced by constraint and image forces that



pull it towards object contours. Snakes are greatly used in applications like object tracking, shape recognition, segmentation, edge detection, stereo matching. Snakes may be understood as a special case of general technique of matching a deformable model to an image by means of energy minimization.

So the Active Contour model for monocular images have been extensively studied and used in many applications such as facial image processing, object tracking and medical imaging. However, the performance of snake models degrades significantly when they encounter challenges such as boundary concavities, object occlusion, and background noise and clutter. Recently, snake-based segmentation methods have been revitalized with the advent of stereo and multi-view imaging technology [1]. An increasing volume of research effort has been focused on combining depth information with snake-based segmentation such as the research of Kim *et al.*. This depth information can be easily extracted from multiple views of the object.

An Active Contour (Snake) is an energy minimizing model guided by internal constraint forces and influenced by external forces which attract it toward features such as lines and edges. In snake-based object segmentation methods, a snake is iteratively attracted to the *OOI* until it converges to its boundary. Snakes are broadly classified into two categories: parametric and geometric. The parametric snake model was first introduced by Kass *et al.* in [4] as an energy minimizing spline. In its discrete formulation, a parametric snake is a set of points  $v_i = (x_i, y_i)$  for  $i=0, \dots, M-1$  where  $x_i$  and  $y_i$  are the  $x$  and  $y$  coordinates of the  $i^{\text{th}}$  snake point respectively, and  $M$  is the total number of snake points. The energy model for the parametric snake is a functional that is typically written as:

$$E_{snake} = \sum_{i=0}^{M-1} (E_{int}(v_i) + E_{ext}(v_i)) \quad (1)$$

The  $E_{int}$  energy term is called the internal energy term, and it is concerned with snake properties such as bending and discontinuity.  $E_{ext}$  is the external energy term and it is usually defined as the gradient of the intensity image.

A major shortcoming of parametric snakes is their inability to proceed into boundary concavities. Some research solutions have been proposed to handle this problem such as the Gradient Vector Flow (GVF) snake proposed by Xu *et al.* in [20].

A geometric active contour [13], also known as geodesic active contour (GAC), is formulated as a curve  $C$  that has a weighted length  $L_g(C)$  such that:

$$L_g(C) = \int_0^1 g(C(p)) |C'(p)| dp \quad (2)$$

Where  $g$  refers to image forces and is defined, similarly to the parametric snake model, in terms of the image gradient as:

$$g = 1 / (1 + |\nabla G_{\sigma} * I|^2) \quad (3)$$

GAC snakes are typically implemented using level set techniques where the snake is embedded as the zero level set of a higher dimensional function, see [13]. This implementation enables GAC snakes to handle boundary concavities and topology changes naturally.

While the GAC model, the GVF model and the various other ACM variants show that the model can be modified to improve its performance against the concavity problem, the background clutter problem remains a challenge which cannot be treated through modifications to the model but rather requires ad hoc treatment.

Our proposed improved stereo correspondence method attempts to help the snake overcome the background clutter challenge via the separation of object edges from background edges, as it gives more accurate and efficient stereo matching procedure

based on multi-level edge maps and the color of the pixel in the stereoscopic pair.

### 1.2.2) Background clutter problem:

As we mentioned earlier that the performance of snake models degrades significantly when they encounter challenges such as boundary concavities, object occlusion, and background noise and clutter.

Background clutter, the focus of this research work, is the existence of various scene components in the background of the image. These components result in noise edges which obstruct the active contour and prevent it from reaching and converging on the *OOI*'s boundary; what is known as the local minima problem, see Figure (1.3). For the snake all edges are the same because it cannot distinguish between edges of the *OOI* and those of other image components, and thus the snake will converge on the first edge in its way.

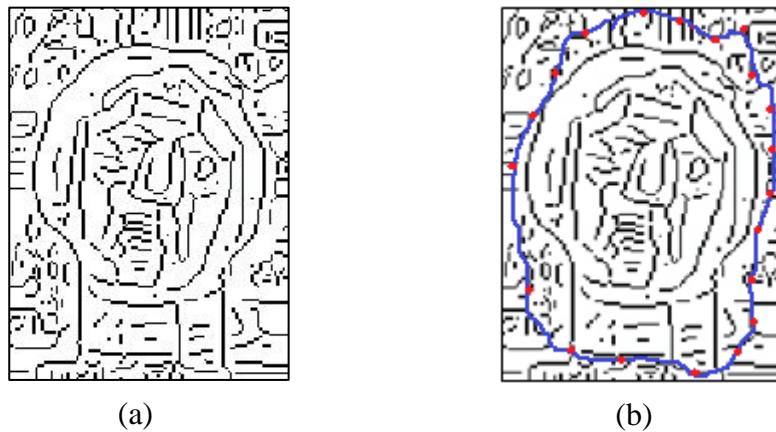


Figure (1.3): The background clutter problem caused by background edges prevents snakes from accurately converging to the object's boundary- (a) without snake, (b) with snake.

The background clutter problem has typically been either avoided or handled using *a priori* shape models [3]. Avoiding background clutter is by initializing the snake as

close to the *OOI* as possible and in a way as to exclude background clutter from the snake's processing field. Obviously, this approach is not suitable for practical purposes as it requires significant manual intervention. In other approaches, *a priori* shape models have been used, such as in [13], to identify the *OOI* and its edges and therefore classify all other edges as background clutter. While such methods may work for specific applications where prior knowledge about the *OOI* is available, obviously they cannot be used outside of their domain.

### 1.2.3) Stereo matching:

Stereo matching is the process of finding corresponding point between two offset images of the same scene. This depth information can be extracted from multiple views of the object. Stereo image pairs are a special case of multi-view images. In stereo, the image pair is captured under the restriction of: same plane, epipolar alignment, limited focal length. As shown in figure (1.4), stereo matching is performed as a pre-processing step in order to identify which pixels within the region of interest ROI belong to the *OOI* and which pixels belong to the background.

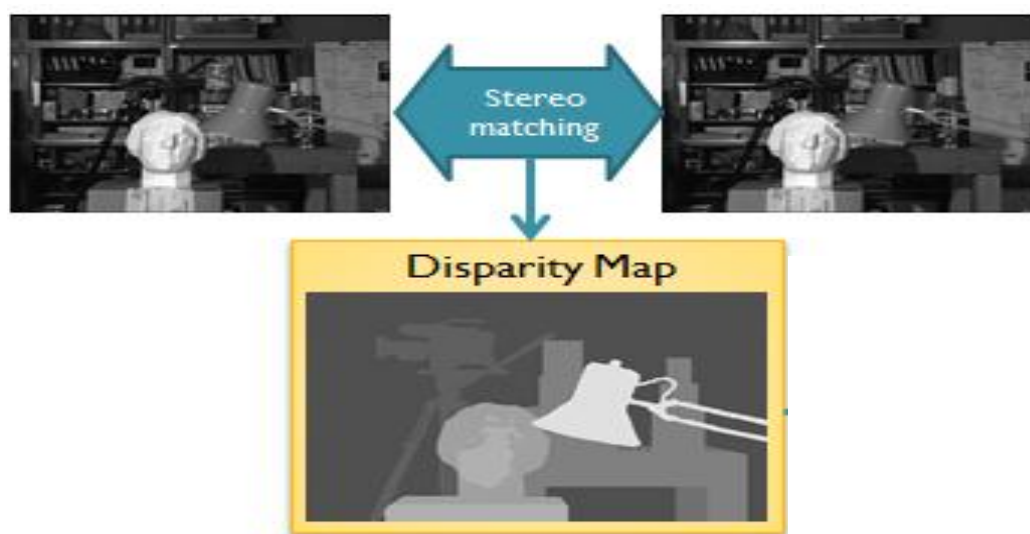


Figure (1.4): Stereo matching approach

In a further step object pixels are preserved while background pixels are eliminated, as shown in figure (1.5), by cleaning the background the snake can operate on a clean background without noise (clutter); ideally.

Although, existing stereo correspondence techniques typically perform well not demonstrate sufficient adequacy for snake-based object segmentation.

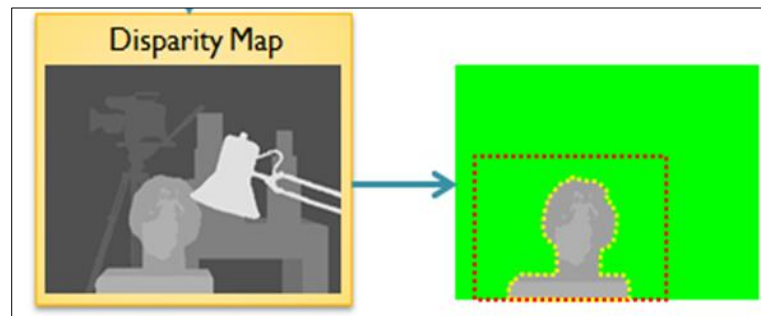


Figure (1.5): preserving object pixels and eliminating background pixels

Stereo correspondence techniques are typically feature-based [7], which means they rely on detecting features, such as edges, corners, lines segments, curve segments, circles etc., which are used as basis for the correspondence procedure. Unfortunately, the detection of most of these features typically incurs high processing overhead especially when a combination of features is adopted. When used in the context of snake-based segmentation, there is an additional waste of processing time because all pixels in the features are matched although only edge pixels are of interest for the snake. Therefore, a more efficient stereo correspondence technique for snake-based segmentation should focus mainly on edges. Figure (2.2) shows the classification of the stereo matching algorithms and there techniques.

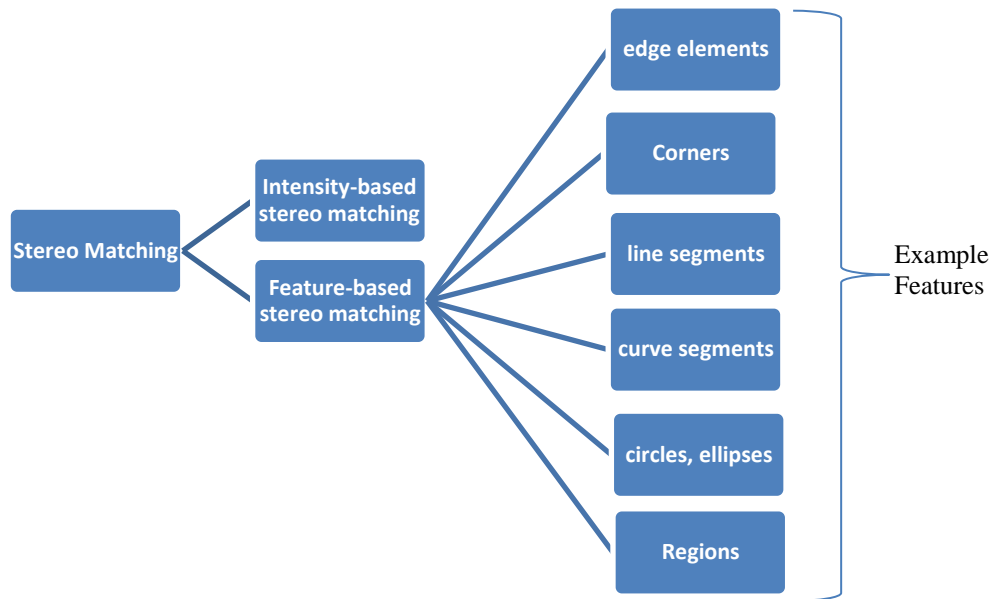


Figure (1.6): Stereo Matching

In conjunction with snake-based object segmentation, the processing overhead problem is further amplified in a variety of likely cases. Region-based stereo matching, for example, after all the time spent in detecting regions will perform stereo matching for all pixels in the *ROI* when only edge pixels are of interest to the snake. Another case is when it turns out that after having consumed time to be detected, some of the features are actually inside the *OOI* and will never be processed by the snake. Moreover, in object segmentation a large portion of objects may not have well-defined geometric features such as corners, lines, curve segments, circles, etc.

Against these shortcomings, edge strength stands out as the more suitable feature to be used as the basis for stereo correspondence for various reasons.

In the following we discuss some of the most common correlation measures used to estimate disparity in stereo correspondence.

### 1.2.3.1) Correlation Measures:

In finding the disparity map of the stereo image pair we depend on the correlation measures to find the disparity map and to use the target localization of the *OOI*, so Correlation based matching typically produces dense depth maps by calculating the disparity at each pixel within a neighborhood. This is achieved by taking a square window of certain size around the pixel of interest in the reference image and finding the homologous pixel within the window in the target image, while moving along the corresponding scanline. The goal is to find the corresponding (correlated) pixel within a certain disparity range that minimizes the associated error and maximizes the similarity.

In brief, the matching process involves computation of the similarity measure for each disparity value, it gives types of the similarity measures; followed by an aggregation and optimization step. Since these steps consume a lot of processing power, there are significant speed-performance advantages to be had in optimizing the matching algorithm.

The images can be matched by taking either left image as the reference (left-to-right matching, also known as direct matching) or right image as the reference (right-to-left matching, also known as reverse matching) [5]. There are many correlation measures used as follows:

- **Sum of Absolute Differences (SAD)**, is one of the simplest of the similarity measures which is calculated by subtracting pixels within a square neighborhood between the reference image  $I_1$  and the target image  $I_2$  followed by the aggregation of absolute differences within the square window, and

optimization with the winner-take-all (WTA) strategy. If the left and right images exactly match, the resultant will be zero.

$$SAD = \sum_{(i,j) \in W} |I_1(i,j) - I_2(x+i, y+j)| \quad (3)$$

- **Sum of Squared Differences (SSD)**, the differences are squared and aggregated within a square window and later optimized by WTA strategy. This measure has a higher computational complexity compared to SAD algorithm as it involves numerous multiplication operations.

$$SSD = \sum_{(i,j) \in W} (I_1(i,j) - I_2(x+i, y+j))^2 \quad (4)$$

- **Normalized Cross Correlation** is even more complex to both SAD and SSD algorithms as it involves numerous multiplication, division and square root operations.

$$NCC = \frac{\sum_{(i,j) \in W} I_1(i,j) \cdot I_2(x+i, y+j)}{\sqrt{\sum_{(i,j) \in W} I_1^2(i,j) \cdot \sum_{(i,j) \in W} I_2^2(x+i, y+j)}} \quad (5)$$

- **Sum of Hamming Distances** is normally employed for matching census-transformed images (can be used on images that have not been census transformed) by computing bitwise-XOR of the values in left and right images, within a square window. This step is usually followed by a bit-counting operation which results in the final Hamming distance score.

$$SHD = \sum_{(i,j) \in W} I_1(i,j) \oplus I_2(x+i, y+j) \quad (6)$$



### 1.2.3.2) Edge-base Stereo matching:

Edge strength stands out as the more suitable feature to be used as the basis for stereo correspondence for various reasons. The more obvious reasons are that edges remain the one type of feature that is guaranteed to exist in all types of objects, and that edges are more relevant to snake-based object segmentation methods because the snake model is simply edge-oriented. Moreover, there are plenty of techniques to detect edges without significant processing cost, compared to detecting other features. In addition, edge strength is a feature that is highly stable under the change of viewpoint, i.e. between left and right, and possible change in strength can be easily handled with a tolerance factor. Furthermore, edge strength is easily quantized into levels which in turn serve as a matching constraint for guiding the matching process [3]. Using stereo matching, the background clutter problem can be handled with the following steps:

- Estimating depth of edge pixels
- Estimating depth of the OOI
- Filtering out all non-OOI edges (clutter edges)

Once clutter edges are eliminated, a snake may be employed to find the OOI's contour.

## **Chapter (2):**

### **Related Works**

This chapter discusses the related works of others in solving the background clutter problem and also in using the stereo matching, where this chapter is divided into two sections. The first section discusses the previous works in stereo matching and snake segmentation, where the second section discusses the previous work of Alattar.

## **2.1) Previous works in stereo matching and snake segmentation:**

Kim *et al.* [2] proposed a new snake-based algorithm for object segmentation in stereo matching. This algorithm first calculates a disparity map using a region-based stereo matching technique. It then uses this disparity map to compute the external energy term of the snake. Given an object of interest (OOI), to estimate its disparity value ( $D_{OOI}$ ), Kim's algorithm calculates a disparity histogram of the region of interest (ROI), then it takes its peak to indicate  $D_{OOI}$ . This method generally works, but it fails when the objects have thin and curved shapes. These objects do not fill up the ROI and hence cause the failure.

Kim *et al.* [9] presented a snake-based scheme for efficiently detecting contours of objects with boundary concavities because of the concavities in the boundary of an object pose a challenge to active contour (snake) methods. The proposed method is composed of two steps. First, the object's boundary is detected using the proposed snake model which says that the movement of snake points is determined using the sign of the cross product of the tangent and normal vectors. Second, snake points are optimized by inserting new points and deleting unnecessary points to better describe the object's boundary. The proposed algorithm can successfully extract objects with boundary concavities, and is insensitive to the number of initial snake points. The researchers say

that their experimental results have shown that the algorithm produces more accurate segmentation results than the conventional algorithm.

As the proposed algorithm produces more accurate segmentation results than the conventional algorithm, to work accurately this algorithm needs a clear background so that the snake segmentation proposed will select the OOI very carefully.

Birchfield and Tomasi [10] presented a method for detecting depth discontinuities from a stereo pair of images. The approach inverts the traditional role of a stereo algorithm because, instead of using the knowledge of depth discontinuities to compute disparity more accurately, they computed a rough disparity map in order to get crisp discontinuities. The algorithm uses a form of dynamic programming to match epipolar scan lines independently, detecting occlusions and depth discontinuities simultaneously with a disparity map. Then a post-processing step propagates information between the scan lines to refine the disparity map and the depth discontinuities. Throughout the process, they used neither windows nor preprocessing of the intensities, thus matching the individual pixels in one image with the pixels in the other image.

As a stereo algorithm, the approach contains three novelties. First, the image sampling problem is overcome by using a measure of pixel dissimilarity that is insensitive to sampling. Secondly, the algorithm handles large untextured regions which present a challenge to many existing stereo algorithms. Finally, unlikely search nodes are pruned to reduce dramatically the running time of dynamic programming. But the performance ( calculation time ) of the stereo matching algorithm proposed is too long compared with other algorithms.

Yean Yin *et al.* [14] presented algorithm which utilizes color mean-shift segmentation on the reference image and local matching based on windows is employed thereafter. A new segment-based dense stereo matching algorithm was given by Lixin Zhang *et al.* [15]. Firstly, the reference view and matching view are over segmented using mean-shift segmentation method. A new region-based approach is proposed to obtain the initial disparity maps of the two views. Then, the unreliable matching points are filtered out by left-right consistency checking technique. An improved greedy search algorithm is applied to propagate the reliable disparity to the segments which don't have reliable disparity. Finally, the disparity map in coarse regions is refined.

Borisagar and Zaveri [11] proposed a novel algorithm that compares disparity map results obtained for Mean shift, Hill climbing, Otsu and Graph-based color segmentation techniques. The color segmentation algorithm has two assumptions. Firstly, disparity values vary smoothly in segmented regions; secondary, depth discontinuities only occur on region boundaries. The purpose of the segmentation is to obtain the segment, as the segment is the base for the consequent analysis. Some segment-based methods are not taking into consideration the quality of segments, which results into inaccurate depth estimation in the poor segmented areas. Different segmentation methods will lead to a huge impact on the accuracy. Firstly, it use the epipolar rectified image pairs as input. For any point in the left image, its matching point will lie on the corresponding horizontal epipolar line. Secondly, as a preprocessing step bilateral filter (A bilateral filter is an edge-preserving and noise reducing smoothing filter) is applied to both left and right images. The intensity value at each pixel in an image is replaced by a weighted average of intensity values from

nearby pixels. This weight is based on a Gaussian distribution. Crucially the weights depend not only on Euclidean distance but also on the radiometric differences. This preserves sharp edges by systematically looping through each pixel and according weights to the adjacent pixels accordingly.

D. Markovic *et al.* [8] presented a method to combine intensity and stereo-derived edges for more reliable recognition of object contours. In experiments with stereo frames it is demonstrated that the implemented Edge Combination algorithm can improve the performance of a GVF snake. In principle, the proposed approach can be applied as a post-processing step to the output of any edge detection and stereo matching algorithm. In the experiment, they utilize stereo-derived depth maps to improve the quality of the snake result so the first step in the method is the Edge Detection which is used to detect edges in both the original image and its corresponding disparity/depth map, then they used what known as Edge Search where the original edge image and the disparity edge image are input to the Edge Combination procedure to determine whether a corresponding edge pixel with a similar orientation can be found in two maps. Because of the imperfect disparity information, some pixels in the comparing process will not match, leaving a gap in the reconstructed contour line, therefor they used an Edge Linking procedure which is implemented to repairs broken edges in the edge combination image where if a continuous edge in the original edge image indicates that the edge segments should be connected, and finally they used what they called the Cleaning process to delete every edge that do not belong to OOI, to use then the snake algorithm very easily.

These methods generally work, but they failed when the objects have thin and curved shapes. These objects do not fill up the ROI and hence cause the failure.

## **2.2) Previous Stereo correspondence method proposed by Alattar:**

The overall approach of Alattar's [3] method is to quantize edge strength into levels, generate multi-level edge maps of the stereoscopic pair, and perform the stereo correspondence procedure under the constraint of edge-strength similarity with some tolerance.

To perform his method, Alattar followed the following steps:

- Generate the Multi-level edge maps from the stereo image pair.
- Generate the edge disparity map by the Stereo Matching depending on the multi-level edge maps.
- Estimate of the OOI's disparity by target localization.
- External energy formulation.

In this section we will explain how [3] applied these steps in his work.

### **2.2.1) Generate the Multi-level edge maps from the stereo image pair:**

Edge strength is a type of similarity constraint but it should not be confused with intensity similarity [16] which merely constrains the matching between pixels to similarity in the intensity value of the pixels. Edge strength, on the other hand, is a measure of the sharpness at which the difference in intensity occurs at the two sides of an edge. While edges are defined as the zero-crossings of the second order derivative of the intensity function, edge strength is basically the magnitude of the first order derivative (gradient) of the intensity function at the edge.

To exploit the edge-strength feature it is necessary to quantize strength into levels so that stereo matching can be constrained to edges of similar strength levels. Furthermore, quantization simplifies the edge strength data and provides a baseline for stereo correspondence.

The basis of the method is the creation of multi-level edge maps of the stereoscopic pair, which allows for imposing the edge strength constraint on the stereo correspondence procedure.

To provide strength information Alattar used the *non-maximum suppression* proposed by [17] is required to suppress, i.e. set to 0, pixels with locally non-maximum strength. He followed the same method used in the Canny edge detector, which calculates an angle  $\theta$  measuring the gradient orientation at a given pixel, and compares the gradient value of that pixel with that of the two pixels on both directions perpendicular to  $\theta$ . For a given pixel, edge orientation is calculated as:

$$\theta = \text{atan} \left( \frac{\partial f / \partial y}{\partial f / \partial x} \right) \quad (7)$$

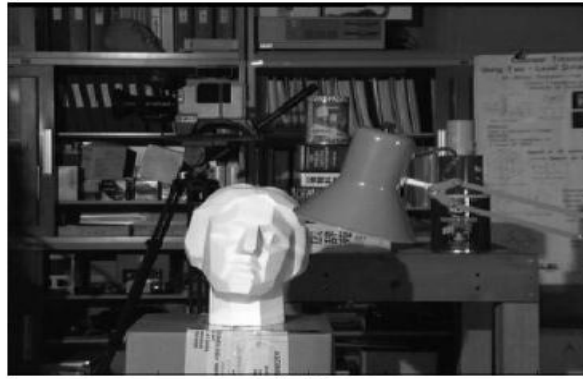
The search is applied within an 8-neighbor window. If the pixel's gradient value is found to be less than the two pixels on both sides, it is suppressed, otherwise it is preserved. This operation produces a gradient edge map,  $g_{edge}(x,y)$ , that can be described by the following expression:

$$g_e(x,y) = \omega \cdot g(x,y) \quad (8)$$

Where  $\omega$  is a local maximum gradient coefficient such that  $\omega=1$  when  $(x,y)$  is a local maximum, and  $\omega=0$  otherwise.

Figure (2.1) shows an image in (a), and presents its gradient magnitude function  $g(x,y)$  in (b), and its edge strength map  $g_{edge}(x,y)$ , in (c) and the Multi-level edge map in (d).





(a)



(b)



(c)



(d)

Figure (2-1): (a) Source image – Tsukuba, (b) gradient magnitude map, (c) Edge strength map –  $(x)$ , (d)

Multi-level edge map

After non-maximum suppression, conventional edge detection methods label pixels based on a threshold value, or two as in the Canny method, to generate a binary edge map. The method, on the other hand, quantizes gradient information, into a smaller set of levels using a set of thresholds. Therefore, by quantization the range of the function  $g_{edge}$ , which ranges from  $0 \rightarrow 255$ , is reduced to a small set of strength levels.

Quantizing edge strength into multi-level edge maps plays an effective role in improving the speed and accuracy of stereo matching.

This speed reduction is illustrated in Figure (2.2). In Figure (2.2) (a), the left and right sides belong to binary edge maps where all edges are indicated by the value 1. Therefore, the left pixel must be matched against all candidate edge pixels on the right side. However, in (b) edge pixels retain their strength value, and thus stereo matching is held only between a pixel on the left against only candidates on the right which have the same or similar strength. As can be seen from Figure (2.2), this has reduced the search from four candidates in (a) to only one candidate in (b).

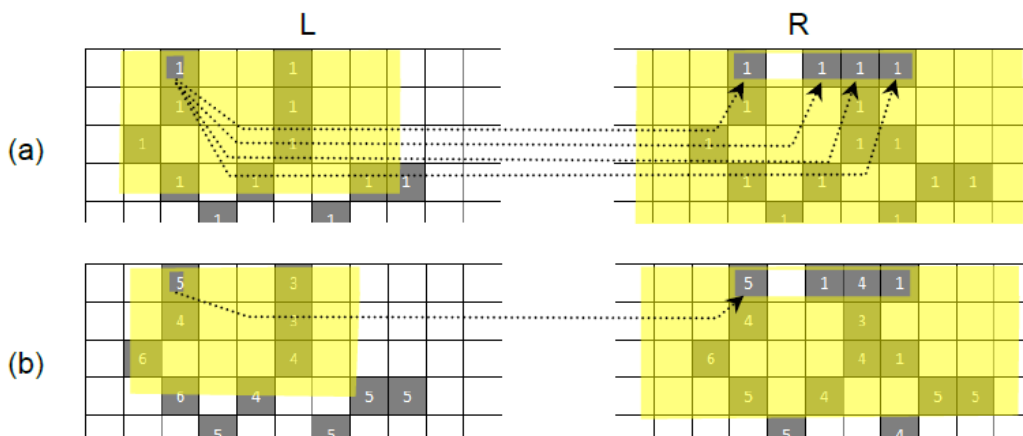


Figure (2.2): Stereo matching search space reduction. (a) The binary edge map case: the left pixel must be matched against all four pixels on the right, (b) The multi-level edge maps case: the left pixel will be matched with only the first pixel on the right

Quantization is achieved based on an equally spaced (uniform distribution) set of intensity thresholds  $Q = \{q\}_{l=1}^N$  where  $N$  is the number of quantization levels and  $q_1=0$ , and  $q_{l-1} < q_l$ . Each pixel in  $(x,y)$  is classified into a level  $l$  if  $q_l \leq(x,y) < q_{l+1}$ . The resulting quantized gradient magnitude map,  $G_{Qmap}$ , is a multi-level edge map, and the procedure is performed for both left and right images. Figure (2.3) presents 3 pairs, (a)-(c), of multi-level edge maps of the Tsukuba image quantized at 4, 8, and 16 levels, respectively.

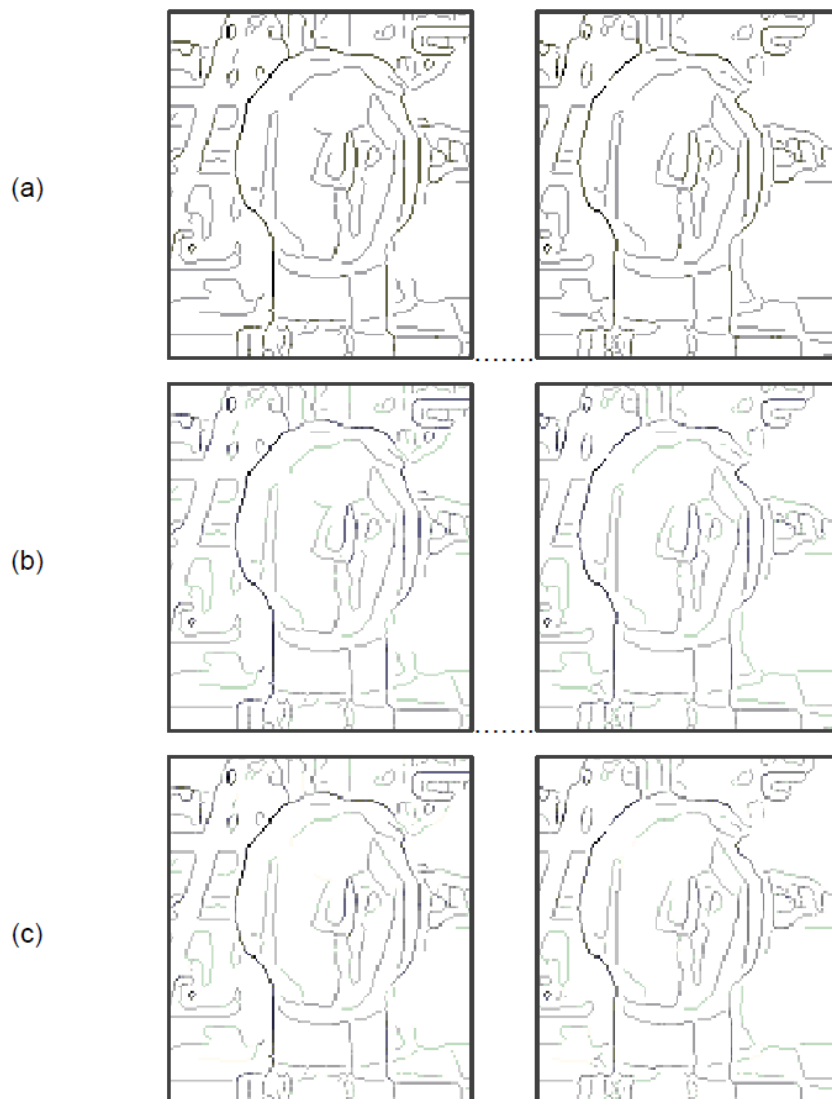


Figure (2.3): (a) 4-level edge map, (b) 8-level edge map (c) 16-level edge map

### 2.2.2) Generating the edge disparity map by Stereo Matching:

For the stereo matching procedure, any matching measure may be used. The commonly used measure can be classified as either correlation-based, or distance-based [17]. Among the correlation-based the most commonly adopted are the Normalized Cross-Correlation (NCC) and the Zero-mean Normalized Cross-Correlation (ZNCC). The most popular distance-based measures are the Sum of Absolute Differences (SAD), and the Sum of Squared Differences (SSD). NCC and ZNCC exhibit good robustness to intensity change, while SSD and SAD show good insensibility towards noise [18], [19]. Since the intensity is not expected to change significantly between the stereoscopic pair, we don't consider intensity change to be a major factor and therefore excluded the correlation-based measures NCC and ZNCC. On the other hand, SAD and SSD offer a more suitable choice for their resilience to noise, and they both produced adequate results. They are defined as follows:

$$\text{SAD}(u) = \sum_{i=1}^n |I_l(x_i, y_i) - I_r(x_i + u, y_i)| \quad (9)$$

where  $I_l$  and  $I_r$  are the left and right images, respectively,  $n$  is the number of candidate pixels in the correlation window, and  $u$  is the  $x$ -displacement.

The matching process also uses a matching technique with a variable window size that depends on edge strength. Since weak edges are typically located within low-textured regions, it is reasonable to expect their correspondence results to be less reliable when a matching window of small size is used. Therefore, they used three window sizes ( $3 \times 3$ ,  $5 \times 5$ , and  $7 \times 7$ ) in inverse proportion to edge strength.

Furthermore, to improve the quality of the output disparity edge map, they adopted a

two-phase stereo matching technique. The mentioned matching process is followed by a second phase that uses a wider window size to re-match any no-matches which may have resulted in the first phase. Figure 2-4 (left) shows an example disparity edge map produced using there stereo matching method.

### **2.2.3) Estimation of the *OOI*'s disparity by target localization:**

Estimating the *OOI*'s disparity ( $D_{OOI}$ ) is an essential element of the method because it provides the basis on which the edge disparity map is filtered for the *OOI*'s edges. Therefore, it is critically important to achieve as accurate an estimate as possible.

A correlation-based similarity search is used to find the best match between edges inside the *ROI* in the left image and those in the right image. To improve performance, this search is limited to edges of the significant levels (weak, strong) only. For  $n$  such edge pixels in the *ROI*, let  $(x_i, y_i)_{i=1 \dots n}$  be the set of their pixel locations, let  $x_0$  be the  $x$ -coordinate of the center of *ROI*, and  $u$  be the  $x$  displacement starting at  $x_0$ . The Sum of Squared Differences (SSD) correlation measure, defined above, is used to estimate the similarity between edge patterns in the *ROI* and candidate edge patterns in the right image. The  $x$  displacement which scores the best correlation determines the best estimate for  $D_{OOI}$ .

### **2.2.4) Snake's external energy formulation:**

In the final step, the edge-based disparity map is filtered to yield an edge map of edges belonging to only the *OOI*. To handle cases of objects with varying disparity values across their surface, we allow a tolerance factor,  $\epsilon$ , in the filtering procedure. We call the resulting edge map a layer edge disparity map (*LEDM*), and it is defined as follows:

$$f_{LEDM}(x,y) = \begin{cases} 1, & \frac{|D_{OOI} - D(x,y)|}{D_{OOI}} < \varepsilon \\ 0, & \text{otherwise} \end{cases} \quad (10)$$

Where  $D(x,y)$  is the disparity map,  $D_{OOI}$  is the object's disparity, and  $\varepsilon$  is a fractional tolerance factor. The edge map shown in Figure (2.4) (right) is an example *LEDM*. Further processing of the *LEDM* map depends on the particular snake model to be used for segmentation. This includes the generation of a gradient map, as in the case of most snake methods, or the generation of a gradient field, as in the case of the GVF snake.

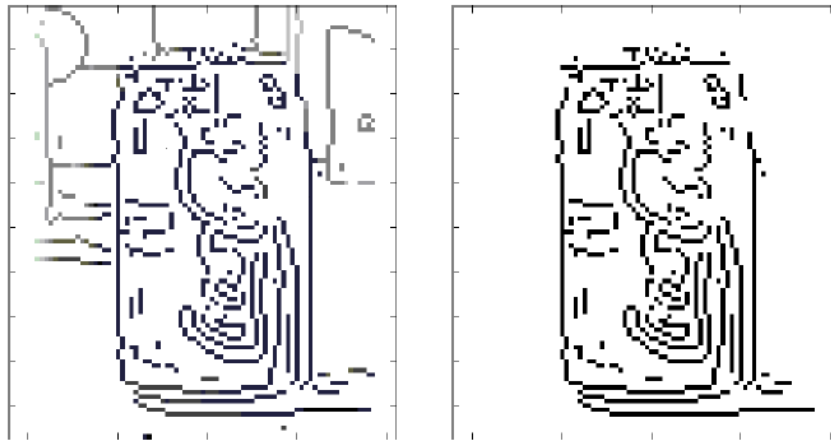


Figure (2.4): Edge Disparity Map (left), and *LEDM* (right)

In Alattar proposed method the accuracy of the of the resulting disparity map for complexes cluttered background image decreases, as the results show some cases where some objects had short gaps in their boundary causing the snake to penetrate these gaps and thus misrepresent the boundary.

In this chapter we discussed the related works of others in solving the background clutter problem and also in using the stereo matching, we also presented the work of

Alattar in more details. However here we pointed out that multi-level edge maps are multi-valued (non-binary) edge maps based on the edge strength.

In the next chapter we discuss our proposed improved stereo correspondence method in more details.

## **Chapter (3):**

# **The Proposed Improved Stereo Correspondence Method**



Our method follows the same approach of Alattar [3], which consists of quantizing edge strength into levels, generating the multi-level edge maps of the stereoscopic pairs and perform the stereo correspondence procedure under the constrain of edge strength similarity.

In our work we improve the work of Alattar [3] in terms of the following steps:

- Modified approach of creating the multi-level edge maps based on 8 levels edge strength of the stereoscopic pair instead of 4 level edge maps to limit the correspondence calculation to respective edges with similar strength.
- Using the color as a factor in calculating the disparity map along with the edge-strength.
- In calculating the disparity map we focused on using two correlation measures which are Sum of absolute deference (SAD) and Sum of square deference (SSD).
- We used a different technique for estimating disparity of the  $OOI$  ( $D_{OOI}$ ).

The main advantage of our work is to increase the accuracy of the edge disparity map and then as a result a more accurate snake segmentation. Our work does not have that big effect on the speed of the processing and that's by reducing the correspondence search space by limiting the correspondence calculation to edges of similar strength and similar color.

Unlike other feature-based methods, our improved method is specifically tailored for snake-based object segmentation, and for that goal it provides a number of advantages which improve snake-based object segmentation in stereo matching. Figure (3.1) depicts the overall modified method.

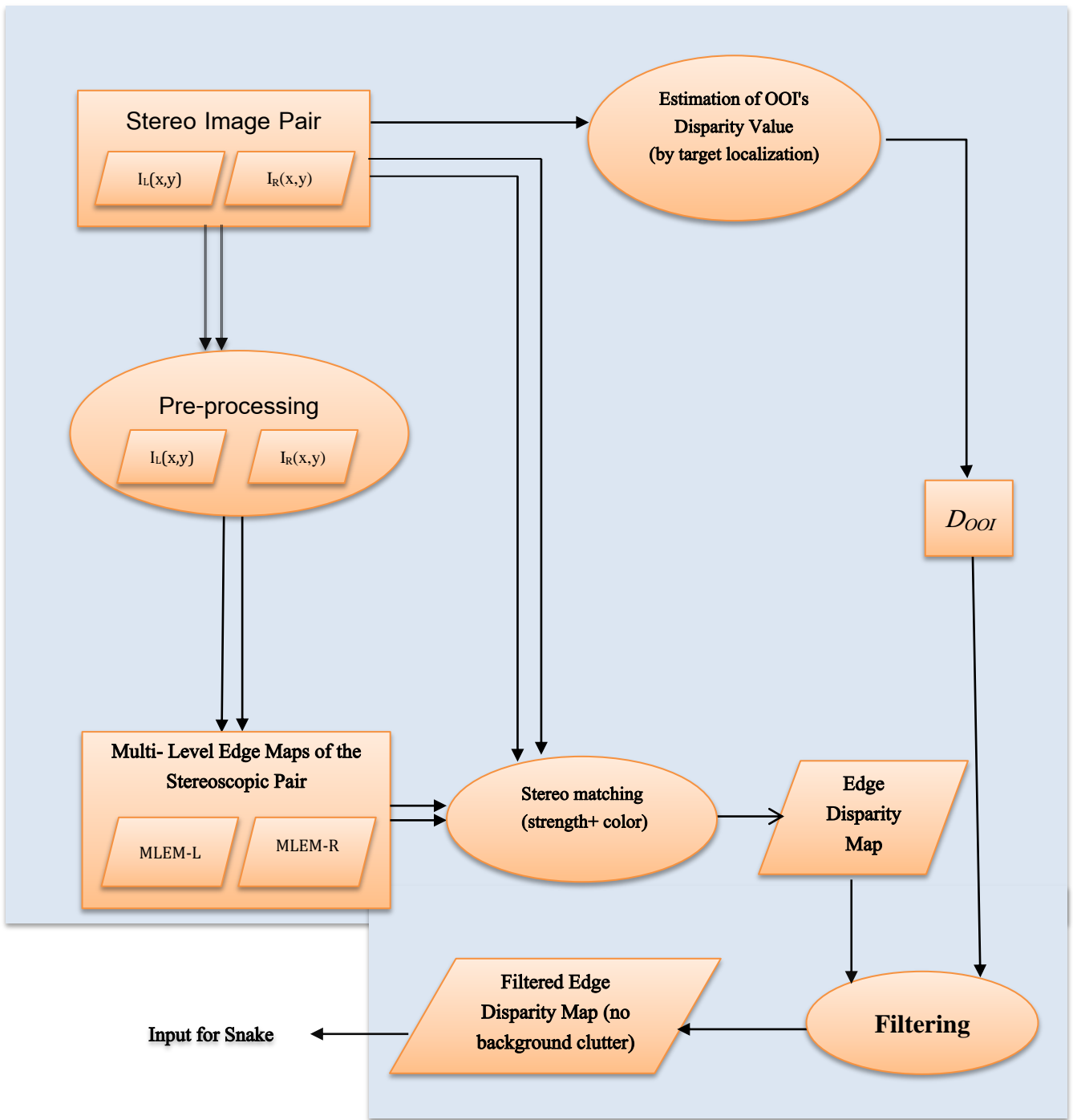


Figure (3.1): Diagram of our Improved Method

As shown in figure (3.1) the modifications I proposed to calculate the edge disparity map are as follows:

- Modify levels (alter the levels to 8 levels).
- Utilize color information in stereo matching step.
- Use two correlation measures (SAD and  $SSD$ ).
- Use a different technique in estimating the  $D_{OOI}$ .

In the following sections we explain the major aspects of our method in further details.

### 3.1) Modifying the multi-level edge map:

The first step in improving the method is modifying the multi-level edge map from 4 level edge maps to 8 level edge maps, which plays an effective role in improving the speed and accuracy of stereo matching as shown in figure (3.2). Where we can reduce the search space as edge pixels retain their strength value, and thus stereo matching is held only between the edge pixel on the left against only candidates on the right which have the same or similar (meaning more than correspondence strength by on or less than it by on) strength.

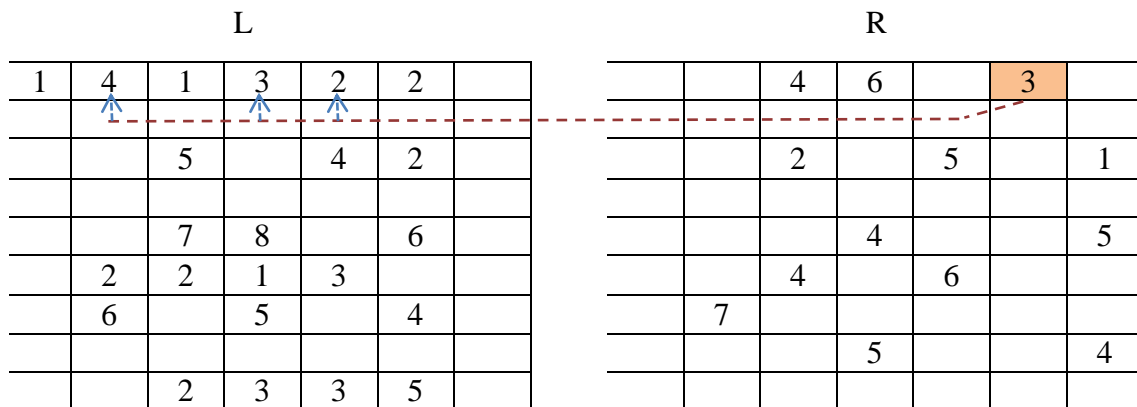


Figure (3.2): Stereo matching search space reduction and accuracy. The multi-level edge maps case: the right pixel will be matched with the pixels that are the same or similar on the left not only with the pixel that is the same.

In generating the multi-level edge maps we quantize edge strength into multi-level edge maps, which plays an effective role in improving the accuracy of stereo matching.

As shown in figure (3.2) edge pixels retain their strength value, and thus stereo matching is held only between a pixel on the left against only candidates on the right which have the same or similar strength.

Quantization is achieved based on an equally spaced (uniform distribution) set of intensity thresholds  $Q = \{q\}_{l=1}^N$  where  $N$  is the number of quantization levels and  $q_1=0$ , and  $q_{l-1} < q_l$ . Each pixel in  $(x,y)$  is classified into a level  $l$  if  $q_l \leq (x,y) < q_{l+1}$ . The resulting quantized gradient magnitude map,  $G_{Qmap}$ , is a multi-level edge map, and the procedure is performed for both left and right images. Figure (3.3) shows the multi-level edge maps for the left and the right ROI for the Tsukuba image.

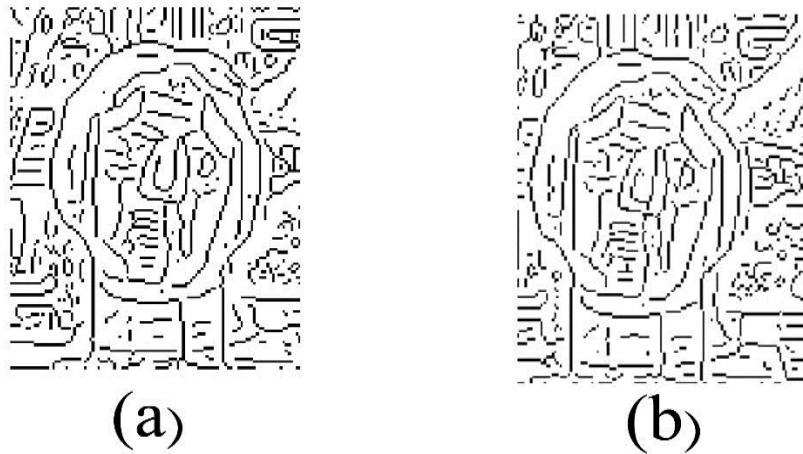


Figure (3.3): 8-level edge map for the Tsukuba image: (a): Right image multi-level edge map, (b): left image multi-level edge map

The main advantage of this modification in this step is to increase the accuracy of the multi-level edge maps by increasing the number of classification of the edges from 4 levels to 8 levels. This plays an important role in increasing the accuracy of the multi-level edge map by making the edges appear in the appropriate level they belong to.

### **3.2) Combing multi-level edge maps and color factor to generate the disparity map:**

The output of the stereo correspondence process is significantly improved with the proposed use of multi-level edge maps and the original colored image. The disparity map is generated based on edge strength along with the use of the color similarities from the original image.

The main advantage achieved from this proposed improved technique is the accuracy of the disparity map which results more accuracy in the use of the snake segmentation by reducing the background clutter.

Although our work has a little effect on the processing speed as with edge-strength levels, the stereo correspondence procedure is limited to edges of similar strength and color, limiting matches within edges of similar strength and color avoids false matches and therefore produces more reliable results.

In generating the disparity map we used the color similarity factor along with the 8 level edge map. Each correspondence edge pixel which has the same edge level or similar to it ( bigger or less than the reference edge pixel by one ) will be entered in another matching process which is the color factor matching process, where we take a  $3 \times 3 \times 3$  window.

The  $(3 \times 3 \times 3)$  kernel is used to take in account the main three colors of the RGB image which are the red, the green and the blue colors from the right original image and then each edge pixel that satisfies the edge matching condition from the multi-level edge map we take its coordinates and go to original left image and take from it a  $3 \times 3 \times 3$  window around the coordinates taking and then apply the matching using one of the correlation measures known.

In our work we used two of the correlation measures which are Sum of Absolute Differences (SAD) and the Sum of Squared Differences (SSD) by using the following equations:

$$SAD = \sum_{(i,j) \in W} |I_1(i, j) - I_2(x + i, y + j)| \quad (3)$$

$$SSD = \sum_{(i,j) \in W} (I_1(i, j) - I_2(x + i, y + j))^2 \quad (4)$$

Then the calculation result which has the smallest value is conserved the highest correlation and is recorded in the disparity map in the same coordinates as the reference right edge pixel. This process is repeated for each edge pixel in the right multi-level edge map.

The disparity map is the result of the stereo matching performed between the two multi-level edge maps and the using of the color factor where the matching is performed as follows, for the right edge reference pixel (R):

- First of all we use the reverse stereo matching technique (using the Right image as the reference image).

- For the right edge pixel (R) we take the edge level value and find its similar value or less than it by one or bigger than it by one in the left image which is in the same row as the right edge pixel, as shown in figure (3.4). As for example, to find the correspondence edge pixel of the reference (which equals 3), we start the matching at the same coordinates as the reference pixel to the left side of the row. The pixel which is similar to the reference pixel (which equal 2, 3 or 4) is taking in the matching.

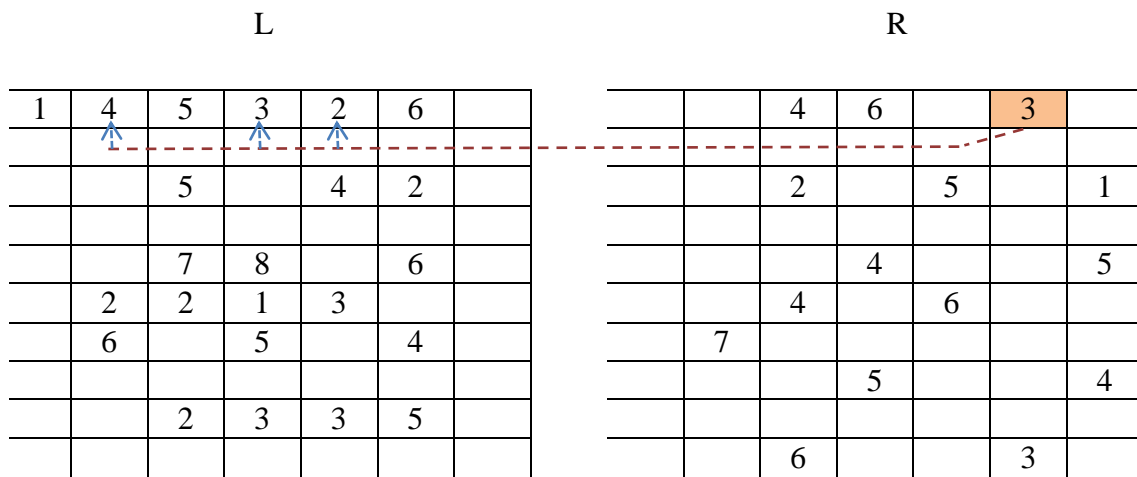


Figure (3.4): Search space reduction and error reduction. The right pixel will be matched with the pixels similar or less or bigger than pixel on the left by one

The coordinates of each pixel that satisfied the matching process is taking and in the original left image we take a  $(3 \times 3 \times 3)$  kernel ( the  $3 \times 3 \times 3$  kernel is used to take in account the main three colors of the RGB image which are the red, the green and the blue colors ) to calculate it's correlation with the  $(3 \times 3 \times 3)$  kernel of the right reference pixel in the original right image and that as shown in figure (3.5).

- Then by using the correlation measures as SAD and SSD and that will be iterated for all the pixels that satisfy the condition. The pixel with the highest

correlation is assumed the corresponded pixel for the reference pixel in the right image and we put in the disparity map the disparity value between the left and the right pixel.

This step is repeated for all the edge pixels in the right image. The result of this step is the creation of the disparity map by depending on the multi-level edge map and color factor of the original image.

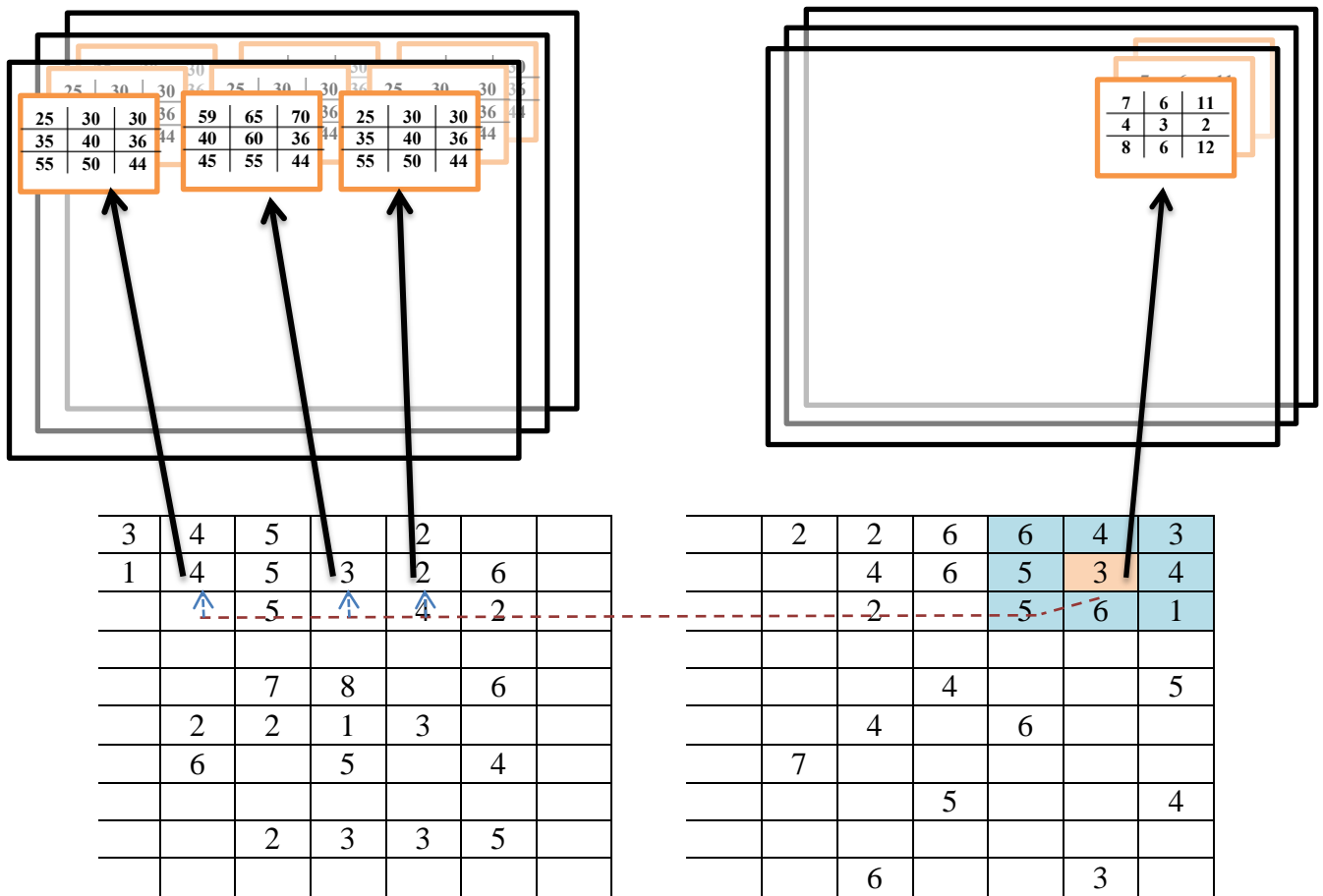


Figure (3.5): Stereo matching using the edge strength value and the color factor of the of the edge pixel in the right image with the edge pixel in the left that satisfies the condition in the left image.



The figure (3.6) shows the ROI of the tsukuba image and its multi-level and color factor disparity map.

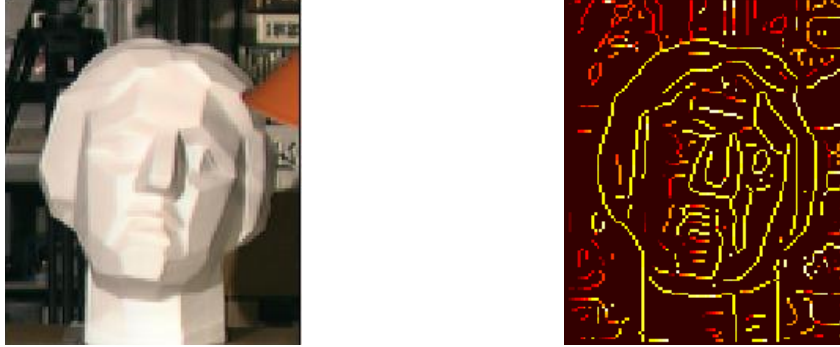


Figure (3.6): The ROI of the tsukuba image and its multi-level and color factor disparity map

### 3.3) Estimation of the *OOI*'s disparity by target localization:

One of the most important steps in our method is estimating the *OOI*'s disparity ( $D_{OOI}$ ) because it provides the basis on which the edge disparity map is filtered for the *OOI*'s edges. Therefore, it is critically important to achieve as accurate an estimate as possible.

To determine the disparity value of the whole *OOI*, we need to calculate the distance between two main points in the left and right images.

One way to find the disparity value is by segmenting the left and right images, and then find the biggest object on the left which will be treated as a mask that has  $X_1$  and  $Y_1$  as the center, then we scan this mask on top of the right to find an object similar to the mask, thus the object with highest similarity exist on the right image has a center of  $x_2$  and  $y_2$ . Now it becomes easy to calculate the disparity value of the whole *OOI* by calculating the difference between  $x_1$  and  $x_2$  ( $abs(x_2-x_1)$ ).

The Bounding Box method is similar to the above method but it does not use the mask approach. As shown in figure (3.7), in bounding box method we separate the objects on

the right and left images by using image segmentation, and then we find the object that has biggest area which is assumed as the *OOI*. We calculate the bounding box of this *OOI*, which is the smallest rectangle that contains all pixels of the *OOI*. Now we determine the center of this box which is  $x_1$  and  $y_1$ . We do the same process on the right image and we calculate the center of the box on the right which is  $x_2$  and  $y_2$ . The disparity value is determined by calculating  $\text{abs}(x_2 - x_1)$ .

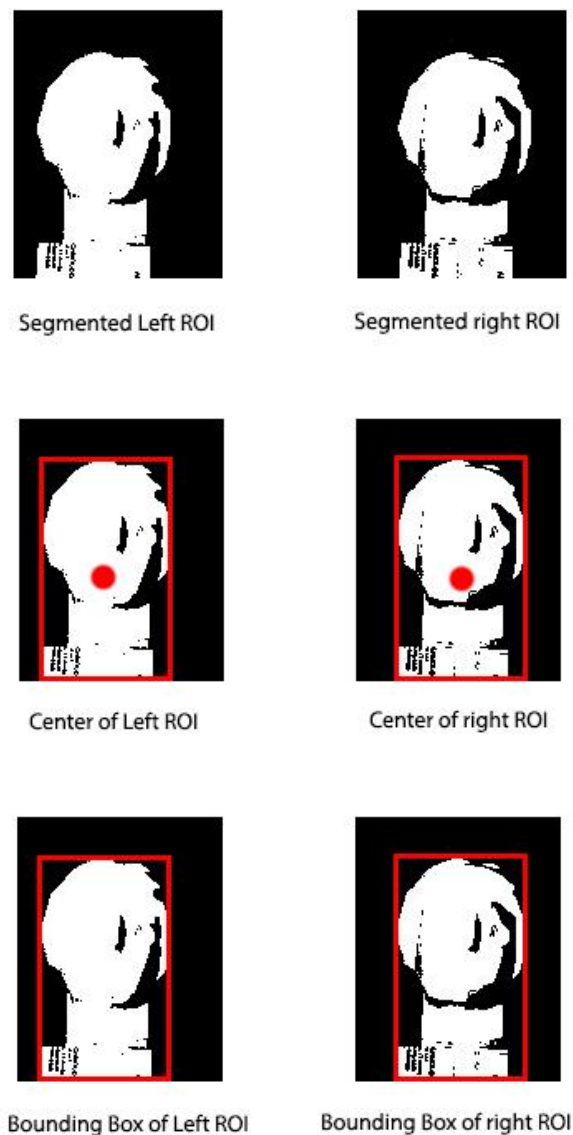


Figure (3.7): the target localization by using the Bounding Box method

The bounding box method is very easy to implement and it is faster than using a mask approach to check for similarity. Figure (3.8) shows the multi-level and color factor disparity map and the layer edge disparity map (*LEDM*) of the Tsukuba ROI.



Figure (3.8): The multi-level and color factor disparity map and the layer edge disparity map (*LEDM*) of the Tsukuba ROI.

### 3.4) Disparity map filtering:

In the final step, we filtered the edge-based disparity map to yield an edge map of edges belonging to only the *OOI*. In this step we followed the same technique as Alattar[3] to handle cases of objects with varying disparity values across their surface, where we used a tolerance factor,  $\varepsilon$ , in the filtering procedure.

The resulting edge map is called a layer edge disparity map (*LEDM*), and it is defined as follows:

$$f_{LEDM}(x,y) = \begin{cases} 1, & \frac{|D_{OOI} - D(x,y)|}{D_{OOI}} < \varepsilon \\ 0, & \text{otherwise} \end{cases} \quad (10)$$

Where  $(x,y)$  is the disparity map,  $D_{OOI}$  is the object's disparity, and  $\varepsilon$  is a fractional tolerance factor. The edge map shown in Figure (3.8) (right) is an example *LEDM*. Further processing of the *LEDM* map depends on the particular snake model to be used for segmentation. This includes the generation of a gradient map, as in the case of most snake methods, or the generation of a gradient field, as in the case of the GVF snake.

At this point we can say that the main problem focused on in this research which is the background clutter problem has been treated but the other problems like gaps and cavities within the object of interest are outside the scope of this research and its performance depends on the design of the snake.

## **Chapter (4):**

# **Experiments and Results**

In this chapter we demonstrate the various experimentations which are performed to evaluate the performance of the proposed improved method, and discuss the results of these experimentations.

These experiments are devised to evaluate the performance of our improved method with respect to the accuracy criterion, which depends on the efficiency in handling background clutter, and for that purpose a set of images with background clutter of degrees varying from slight to intense has been selected for testing our improved method.

To quantify the accuracy of our improved multi-level disparity map method we use the absolute difference which calculates the mean error between a manually defined correct object of interest and the filtered disparity map as follows:

$$\text{Error score} = \sum_i^N |F_i - M_i| \quad (11)$$

Where  $F_i$  is the edge pixel in the filtered disparity map,  $M_i$  is the same coordinate's edge pixel in the manually filtered OOI, and  $N$  is number of pixels.

We implemented our proposed improved stereo correspondence method using MATLAB and the experiments have been executed on an Intel Core 2 Due machine running at 2.20 GHz clock speed with 4 GB RAM. All images used have a 240x320 resolution, unless otherwise indicated. The remainder of this chapter explains the different test cases and presents their results.

The cases are organized in three types which are synthesized images, real indoor images, and real outdoor images, and for each case we used clear background images, moderately cluttered background and highly cluttered background.

For each experimental set, the generated results images are:

- a) Edge maps (for Multi-level and improved Multi-level)
- b) Edge Disparity Maps (for Multi-level and improved Multi-level edge maps),
- c) Filtered edge disparity map.
- d) Error scores (for Multi-level and improved Multi-level edge maps).

**The 1<sup>st</sup> image:**

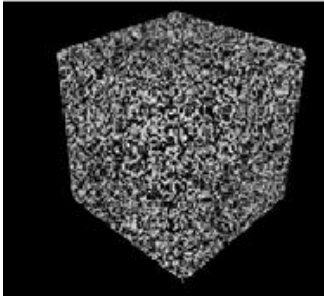
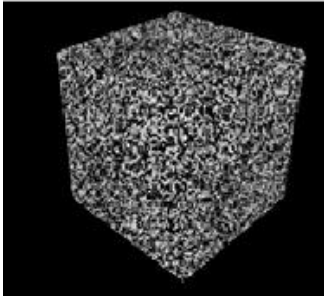
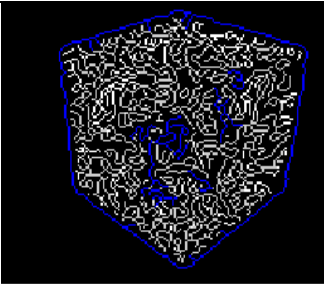
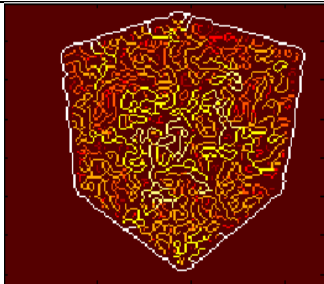
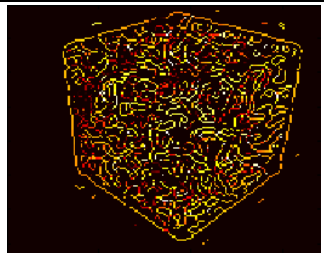
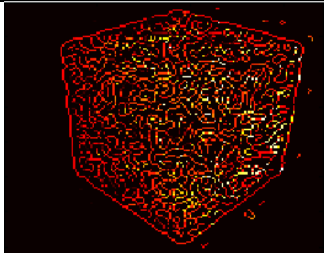


	Alattar Method	Our improved Method
<b>ROI</b>		
<b>Multi-level edge map</b>		
<b>Disparity map</b>		
<b>Filtered disparity map</b>		
<b>Error score</b>	<b>12.3732</b>	<b>11.5578</b>

Figure (4.1): Results for synthesized clear background images

From figure (4.1) shown above we can see that, the performance of our method is only slightly better because the background has clear background.



The 2<sup>nd</sup> image:



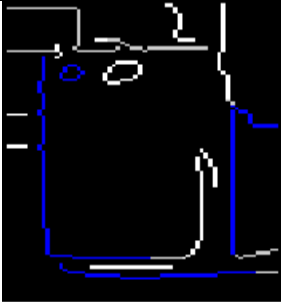

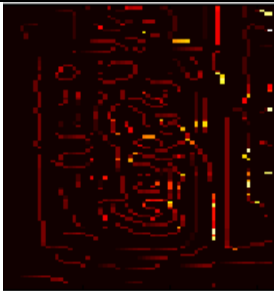
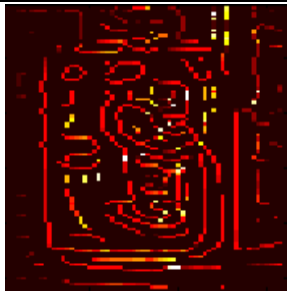




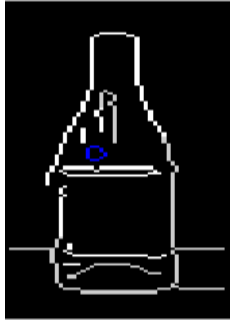
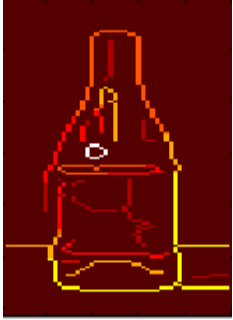
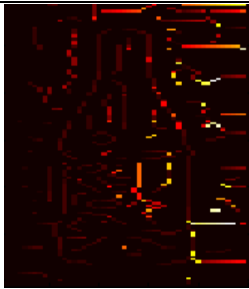

	Alattar Method	Our improved Method
<b>ROI</b>		
<b>Multi-level edge map</b>		
<b>Disparity map</b>		
<b>Filtered disparity map</b>		
<b>Error score</b>	<b>6.85096</b>	<b>6.38522</b>

Figure (4.2): Results for real indoor moderately cluttered background images

As can be seen from figure (4.2), our method shows higher performance than Alattar case as more background edges have been eliminated in our case which resulted in a higher performance by the snake.

**The 3<sup>rd</sup> image:**

	Alattar Method	Our improved Method
<b>ROI</b>		
<b>Multi-level edge map</b>		
<b>Disparity map</b>		



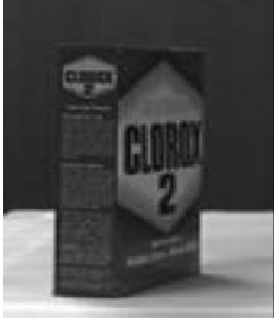



<b>Filtered disparity map</b>		
<b>Error score</b>	<b>5.16393</b>	<b>2.29508</b>

Figure (4.3): Results for real indoor clear cluttered background images

Again as shown in figure (4.3), our method shows higher performance and accuracy than Alattar case which makes easier on the snake to select the OOI more correctly.

#### The 4<sup>th</sup> image:

	<b>Alattar Method</b>	<b>Our improved Method</b>
<b>ROI</b>		
<b>Multi-level edge map</b>		

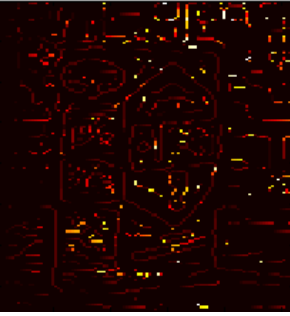


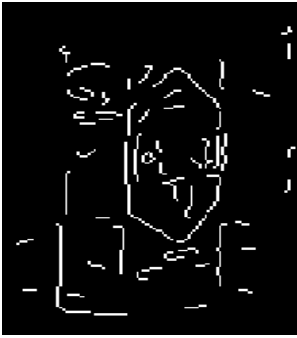
<b>Disparity map</b>		
<b>Filtered disparity map</b>		
<b>Error score</b>	<b>5.34539</b>	<b>3.73229</b>

Figure (4.4): Results for real indoor slightly cluttered background images

Again our method showed a higher performance than Alattar case and that's because our improved stereo matching process produced a better filtered image with less background edges.

**The 5<sup>th</sup> image:**



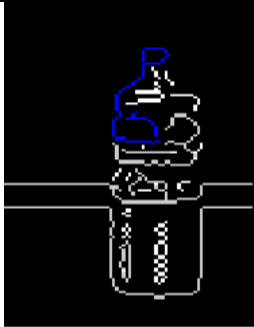



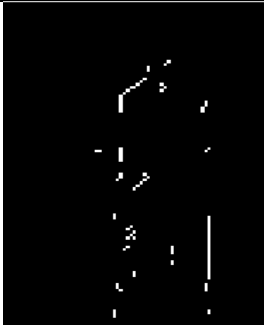
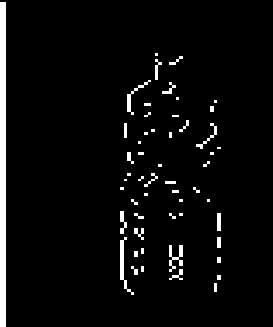




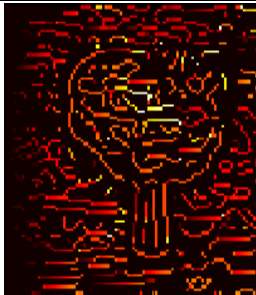
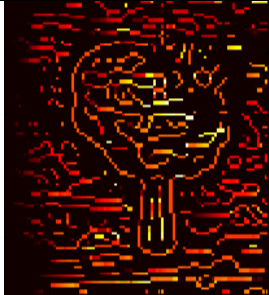
	Alattar Method	Our improved Method
<b>ROI</b>		
<b>Multi-level edge map</b>		
<b>Disparity map</b>		
<b>Filtered disparity map</b>		
<b>Error score</b>	<b>1.41941</b>	<b>1.83755</b>

Figure (4.5): Results for real indoor cluttered background colored images

As we can see from figure (4.5), although our method has more edge pixel from the inside it gave as a more accurate clear background around the OOI.

**The 6<sup>th</sup> image:**

	Alattar Method	Our improved Method
<b>ROI</b>		
<b>Multi-level edge map</b>		
<b>Disparity map</b>		







<b>Filtered disparity map</b>		
<b>Error score</b>	<b>3.80038</b>	<b>1.9602</b>

Figure (4.6): Results for synthesized cluttered background image

From the results of figure (4.6) we find that our proposed method has a more accurate filtered edge disparity map, as for the edge that appear in the filtered map because of the clutter has the same disparity/depth as the object of interest.

### The 7<sup>th</sup> image:

	<b>Alattar Method</b>	<b>Our improved Method</b>
<b>ROI</b>		
<b>Multi-level edge map</b>		

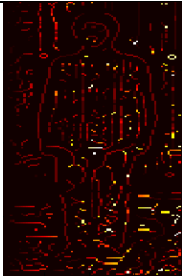





<b>Disparity map</b>		
<b>Filtered disparity map</b>		
<b>Error score</b>	<b>3.57375</b>	<b>1.7154</b>

Figure (4.7): Results for real outdoor slightly cluttered background images

Again our improved method in figure (4.7) showed highly performance results which makes it more easier and accurate for the snake to select the object of interest.

### The 8<sup>th</sup> image:

	<b>Alattar Method</b>	<b>Our improved Method</b>
<b>ROI</b>		



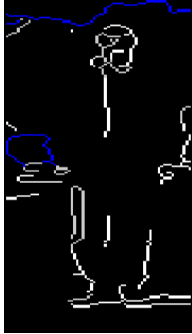

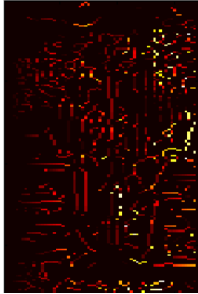
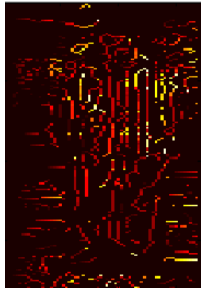


<b>Multi-level edge map</b>		
<b>Disparity map</b>		
<b>Filtered disparity map</b>		
<b>Error score</b>	<b>6.4951</b>	<b>5.04085</b>

Figure (4.8): Results for real outdoor moderately cluttered background images

The filtered edge map of our method performed better results because our stereo matching process produced better filtered image with less background edges.

9<sup>th</sup> image:





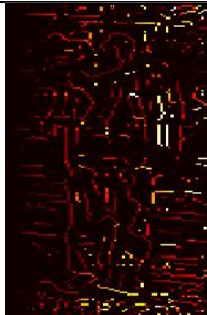





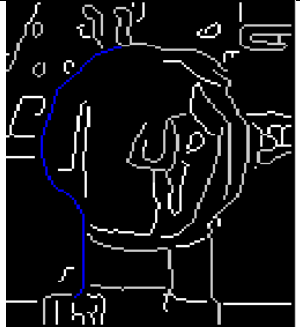



	Alattar Method	Our improved Method
<b>ROI</b>		
<b>Multi-level edge map</b>		
<b>Disparity map</b>		
<b>Filtered disparity map</b>		
<b>Error score</b>	<b>6.12186</b>	<b>4.53047</b>

Figure (4.9): Results for real outdoor highly cluttered background images

Last but not least, in this case the performance of our improved method was better than in the original multi-level edge map stereo matching method because our method eliminated more background edges.

**The 10<sup>th</sup> Image:**

	<b>Alattar Method</b>	<b>Our improved Method</b>
<b>ROI</b>		
<b>Multi-level edge map</b>		
<b>Disparity map</b>		





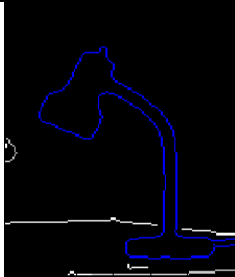

<b>Filtered disparity map</b>		
<b>Error score</b>	<b>4.86886</b>	<b>3.00</b>

Figure (4.10): Results for real indoor highly cluttered background images

As shown in figure (4.10), our method showed a highly accurate filtered edge map by eliminating all unnecessary edges outside the object of interest and as for the gaps and cavities it depend on the performance of the snake.

### The 11<sup>th</sup> image:

	<b>Alattar Method</b>	<b>Our improved Method</b>
<b>ROI</b>		
<b>Multi-level edge map</b>		

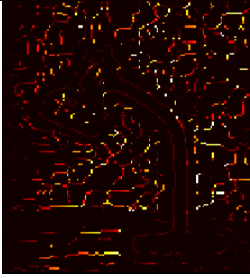


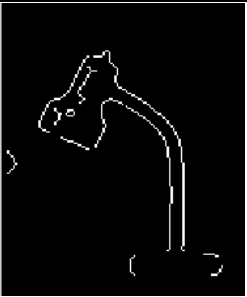


<b>Disparity map</b>		
<b>Filtered disparity map</b>		
<b>Error score</b>	<b>2.26116</b>	<b>0.738744</b>

Figure (4.11): Results for real indoor cluttered background images

Again as shown in figure (4.11), the performance result of our improved multi-level stereo matching method showed a highly accurate filtered disparity map than Alattar case which makes more easier for the snake to select the OOI more accurately.

**The 12 image:**

	<b>Alattar Method</b>	<b>Our improved Method</b>
<b>ROI</b>		

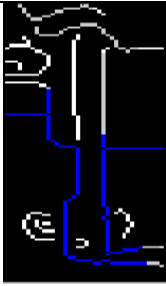

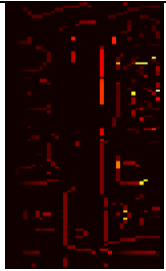
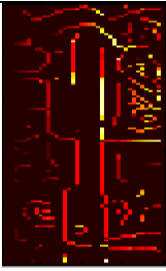
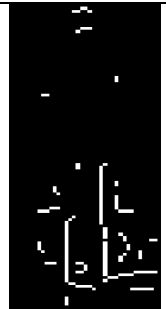
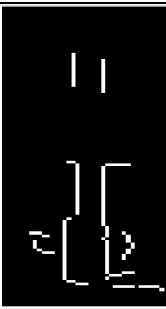
<b>Multi-level edge map</b>		
<b>Disparity map</b>		
<b>Filtered disparity map</b>		
<b>Error score</b>	<b>4.02381</b>	<b>2.40479</b>

Figure (4.12): Results for real indoor cluttered background images – small *OOI*

Again as shown in figure (4.12), although our method eliminates more unnecessary edges outside the *OOI* it still didn't appear the top side of the object of interest which makes selecting it accurately by the snake more difficult.

## **Chapter 6:**

## **Conclusion**

As can be seen clearly from the results in Chapter (4), our improved multi-level stereo matching method have produced better edge-based disparity maps which leads to higher detection accuracy by the snake. Overall, we can make the following remarks:

- As shown in the results real indoor images scored the highest performance due to better lighting conditions, and to suitable focal distance.
- As for the other issues as boundary gaps and cavities within the object of interest depend on the performance of the design of the snake used.
- The researcher can argue that the cavities is not related to the background clutter problem, where the background can be free from clutters however the snake cannot go deeply inside the cavity and this depends on the flexibility of the snake used.
- As for the gaps problem which is the result of having areas that have a very weak in the frame edges of the object of interest, and this is another problem outside the scope the proposed method because the increasing of the number of levels is not expected from it to solve the problem of the weakness of the edges.
- As for the multiple objects detection (when more than one object are of interest is for segmentation): our improved method is similar in utility to other methods which follow the same approach because this type of methods follows a single-object procedure where the method must estimate the disparity of that *OOI* and must delete all other components of the image, therefor to solve this issue by using this type of method we have to process it for each object of interest separately.
- As a future work, various correlation measures, other than SAD and SSD, may be tried to generate the disparity map.



## REFERENCES

- [1] Alattar A. M. and Jang J. W, " A new stereo correspondence method for snake-based object segmentation " , IEEE ICIP 2007, pp. 381 – 384, 2007.
- [2] Kim, S. H., J. W. Jang, and J. H. Choi. "Object Segmentation Algorithm Using Snakes in Stereo Images", Optical Engineering, vol. 45, no. 3, pp. 37-39, Mar. 2006.
- [3] Alattar A. M., "A Multi-Level Edge-Based Stereo Correspondence Method for Snake-Based Object Segmentation", Graduate School of PaiChai University, pp. 13-29, December 2008.
- [4] Kass, M., A. Witkin, and D. Terzopoulos. "Snake: Active Contour Models." Int'l J. Computer Vision, vol. 1, no.4, pp. 321-331, 1987.
- [5] Kanade T., Kano H., and Kimura S., "Development of a video-rate stereo machine," in Image Understanding Workshop, Monterey, CA, pp. 549–557, 1994.
- [6] Scharstein D. and Szeliski R., "A taxonomy and evaluation of dense two-frame stereo correspondence algorithms," International Journal of Computer Vision, vol. 47, pp. 7-42, Apr. 2002.
- [7] [http://homepages.inf.ed.ac.uk/rbf/CVonline/LOCAL\\_COPIES/OWENS/LECT11/node5.html#SECTION00052100000000000000](http://homepages.inf.ed.ac.uk/rbf/CVonline/LOCAL_COPIES/OWENS/LECT11/node5.html#SECTION00052100000000000000), visited in 25th April, 2013.
- [8] Markovic D., and Gelautz M., " Experimental combination of intensity and stereo edges for improved snake segmentation " , Pattern Recognition and Image Analysis Volume 17, Issue 1, pp 131-135, 2007.
- [9] Kim, Shin-Hyoung, Alattar, A. M., Jang, Whan, " A Snake-Based Segmentation Algorithm for Objects with Boundary Concavities in Stereo Images " , IEEE 2006 International Conference on Computational Intelligence and Security, Volume 1, pp 645- 650, 2006.

- [10] Birchfield, Stanley T. ; Tomasi, Carlo, " Depth Discontinuities by Pixel-to-Pixel Stereo ", IEEE Sixth International Conference on Computer Vision, pp 1073 – 1080, 1998.
- [11] Viral H. Borisagar, Mukesh A. Zaveri, " A Novel Segment-based Stereo Matching Algorithm for Disparity Map Generation ", 2011 International Conference on Computer and Software Modeling IPCSIT ,vol.14, pp 25 – 29, 2011.
- [12] [http://en.wikipedia.org/wiki/Active\\_contour\\_model](http://en.wikipedia.org/wiki/Active_contour_model), visited on 25th April, 2013.
- [13] Malladi, R., J. A. Sethian, and B. C. Vemuri. "Shape modeling with front propagation: A level set approach," IEEE Trans. Pat. Anal. Mach. Intell., vol. 17, no. 2, pp. 158-175, June 1995.
- [14] Miao J., Yean Yin S., "A Stereo Pairs Disparity Matching Algorithm by Mean-Shift Segmentation," in Third International Workshop on Advanced Computational Intelligence, pp. 639-642, 2010.
- [15] Yang D., Zhang Z., "A Segment-Based Dense Stereo Matching Algorithm," in Second International Symposium on Information Science and Engineering, pp. 574-578, 2008.
- [16] Grimson, W. E. L. From Images to Surfaces: A Computational Study of the Human Early Visual System; MIT Press: Cambridge, MA., 1981.
- [17] Canny, J., "A computational approach to edge detection," IEEE Trans. Pattern Anal. Mach. Intell., Vol. 8, no. 6, pp. 679-698, November 1986.
- [18] Aschwanden P., and Guggenbuhl W., " Experimental results from a comparative study on correlation-type registration algorithms ". In W. Forstner and S. Ruwiedel, editors, Robust computer vision, pp. 268–289, 1992.
- [19] Martin J., and Crowley J., "Experimental comparison of correlation techniques," In Proc. Int. Conf. on Intelligent Autonomous Systems, vol. 4, pp. 86–93, 1995.

- [20] Koschan, A. "A comparative study on color edge detection," Proceedings, 2nd Asian Conf. on Computer Vision, pp. 574-578, 1995.
- [21] Osher S., and Fedkiw R., " Level Set Methods: An Overview and Some Recent Results ", Stanford University, California, Sep. 2000.
- [22] Sezgin M ., and Sankur B., " Survey over image thresholding techniques and quantitative performance evaluation ", Journal of Electronic Imaging 13(1), pp. 146–165, January 2004.